A New Fluid/Structure Coupling Algorithm for the LMFBR Containment Code SEURBNUK/EURDYN

B.L. Smith
Swiss Federal Institute for Reactor Research, CH-5303 Würenlingen, Switzerland

ABSTRACT

A semi-implicit coupling algorithm is developed which provides a stable interface between the implicit Eulerian hydrodynamics code SEURBNUK and the explicit Lagrangian structure dynamics code EURDYN.
Accelerations at each structural node are divided into two parts: those deriving from the fluid (or gas) pressure and those due to body and internal structural forces. The accelerations are used to update the nodal velocities, implicitly for the pressure-derived component, explicitly for the others. The resulting semi-implicit coupling is demonstrated stable and accurate using a number of one-dimensional tests in both radial and axial geometry. The commonly used explicit (or weak) coupling, though easy to implement in the codes, is shown to be unstable in these circumstances.

1. INTRODUCTION

SEURBNUK is a 2D (axisymmetric) fluid dynamics code developed for use in LMFBR containment studies, /1/, /2/, /3/. An implicit finite difference algorithm similar to ICE /4/, is used to compute the fluid motions with structure response capability provided by a built-in finite difference thin shell model. Appropriate logic exists for handling fluid-structure interaction effects.

The structural modelling capabilities have been enhanced considerably by replacing the thin shell model by a coupling to the finite element structures code EURDYN /5/, /6/. At present two axisymmetric elements from the EURDYN library are accessed: a two-node thin shell element and a three-node triangular element. Some applications of the coupled code SEURBNUK-EURDYN have been reported previously /3/.

Originally, an explicit or weak coupling algorithm, /7/, was used to link the fluid and structure modules in SEURBNUK-EURDYN. Output from the fluid calculation in SEURBNUK gives pressures to be used as boundary conditions for the structure calculation to be performed in EURDYN. Computed structure velocities are then used as boundary conditions for the fluid calculation at the next time step. Accordingly, the fluid and structure motions are not stricly coupled, merely interfaced successively, step by step. In addition, the process is not fully self consistent: the implicit fluid calculation in SEURBNUK (and ICE) requires end-of-cycle velocities at the boundaries, but for the structures, EURDYN supplies only start-of-cycle values.

Nevertheless, similar weak couplings have been used successfully. The code ICECO /8/,

although different in some details to SEURBNUK, is also based on the ICE algorithm and has been coupled in a like manner to WHAM / 9 /, a finite element code very similar to EURDYN. The ICECO-WHAM, SEURBNUK-EURDYN combinations have proved their worth in a variety of fluid-structure situations but the rarity of evidence of instability problems may be fortuitous and misleading. The forward time differencing incorporated in ICE entails a considerable amount of positive numerical diffusion. For compressible fluid calculations any source of instability at a fluid-structure boundary is usually resisted by large structural restoring forces which set up an oscillation propogating through the fluid and damped by the numerics.

A one dimensional test problem is defined in the next Section which provides a very stringent test of the fluid-structure coupling - there are no restoring structural forces and no damping due to fluid compressibility. It is shown that the explicit coupling algorithm in SEURBNUK-EURDYN leads to immediate instability. A new semi-implicit coupling is proposed in Section 3 and shown in Section 4 to lead to a stable solution for this and other one-dimensional test examples. Comparison of results with exact analytical solutions is also given.

2. THE FREE-DISC PROBLEM

The test geometry is given in Figure 1 and comprises a shock tube arrangement with a slug of liquid separating high pressure and low pressure gas regions. A thin steel disc, not supported by the tube, is placed at midway across the liquid column and the motion is followed for increasing time. The liquid is considered incompressible for this test and appropriate linear equations of state are chosen for the gas regions to give harmonic motion.

Thin shell theory is used for the disc and since the liquid regions are incompressible they will move, together with the disc, as a single body. At each time interval the liquid-gas interfaces must move identically with the disc, the pressure drop across the disc being such as to drive the disc at the correct speed. There are no physical stabilising factors if mismatch occurs.

The pressure behind the disc calculated using the explicit coupling in SEURBNUK-EURDYN is shown as the dotted line in Figure 1b. There is seen to be immediate instability leading to code failure after five fluid time steps.

The instability arises from a mismatch of the velocity boundary conditions during the fluid calculation. At time $t = 0$ everything is at rest with the disc velocity, $v = 0$, used as a boundary condition for the first fluid time step. As the fluid is incompressible the only consistent solution is zero pressure gradient everywhere, the disc separating two regions of constant pressure. For the parameters chosen these are 8.8MPa and 0.0MPa, the respective gas pressures.

In reality, the pressure gradients are linear through the liquid slugs, the pressures on the upstream and downstream faces of the disc being respectively 4.8 and 4.0 Mpa. The calculation therefore exaggerates the pressure drop by more than a factor 10 and over-accelerates the disc during the structure calculation. This leads to over-compensation by the fluid pressures at the next time step and in the absence of adequate damping mechanisms the oscillations become ever more violent.

The stable solution shown in Figure 1b results from a calculation performed using the semi-implicit fluid-structure coupling algorithm described in the next Section.

3. NEW COUPLING ALGORITHM

In SEURBNUK the fluid dynamic equations, neglecting viscous forces, are solved in cylindrical geometry by a finite difference procedure based on ICE /4/. An interlaced network of dependent variables is introduced, Figure 2, in which the scalar field quantities, pressure p, density ρ, energy E, are defined at the mesh centres and momenta m, and velocities v, at the cell edges. Using the control volume approach we may write the mass conservation equation for the central cell in Figure 2 in the form

$$\frac{\rho^* - \rho}{\Delta t} = (A_1 m_1^* - A_3 m_3^*)\Delta r + (A_2 m_2^* - A_4 m_4^*)\Delta z \qquad (1)$$

with

$$A_1 = \frac{r_-}{\bar{r}\Delta r^2}, \quad A_3 = \frac{r_+}{\bar{r}\Delta r^2}, \quad A_2 = A_4 = \frac{1}{\Delta z^2}$$

and the asterisk * denoting updated, end-of cycle values.

The control volume for the momenta is offset from the basic cell configuration, as indicated by the dotted line in Figure 2. For the volume shown we may express momentum conservation in the form

$$\frac{m_1^* - m_1}{\Delta t} = \frac{p_1^* - p^*}{\Delta r} + \xi_1 \qquad (2)$$

where ξ_1 represents the advection terms. Similar expressions pertain for the other cell momenta m_2^*, m_3^*, m_4^*. Note the use of updated momenta and pressures in Equations (1), (2). Instead of using the energy equation, the conservation equations (1), (2) are closed using an adiabatic approximation for the equation of state of the fluid. Thus we have

$$(\rho^* - \rho) = C(p^* - p) \qquad (3)$$

where the quantity C is related to the sound speed in the material, updated at the end of each time step. The energy equation proper is used as a check on the approximations used.

Combining (1), (2), (3) leads to an implicit equation for the pressures of the Poisson type

$$p^* = A_1 p_1^* + A_2 p_2^* + A_3 p_3^* + A_4 p_4^* + R \qquad (4)$$

with the source term R evaluated in terms of known quantities /1/.

The pressure equation (4) is solved by iteration for all internal cells. A modified form of the equation may be formulated for use in cells containing (or near) structure boundaries. A typical structure boundary cell is shown in Figure 3. The orientation of the structure surface with respect to the Eulerian grid is described by a piecewise linear curve ABCDE drawn between successive EURDYN nodes on the fluid-structure interface. In the example chosen the fluid is on the left of the structure, shaded in the Figure. If the boundary represents a thin shell or plate there is also fluid on the right and, to include this case, we adopt the terminology p_L and p_R to denote the respective face pressures. If the structure is thick, $p_R = 0$.

A free slip boundary condition is used in SEURBNUK. Thus for end-of-cycle values,

$$u_n^* = U_n^* \qquad (5)$$

where u_n^* is the fluid normal velocity and U_n^* is the structure normal velocity at the interface. Strictly, this relation should be imposed at every point on the boundary, or at least at every node where the structure velocity is known. In practice the presence of the moving structure is communicated to the fluid in an average sense, as described below. Using (5) the mass balance condition for the fluid in the cell, shaded in Figure 5, becomes

$$\frac{\rho^* - \rho}{\Delta t} = (d_1 A_1 m_1^* - A\rho\bar{U}^*)\Delta r + (d_2 A_2 m_2^* - d_4 A_4 m_4^*)\Delta z \qquad (6)$$

in which d_1, d_2, d_4, A are geometric factors depending on orientation, and $\bar{U}^*$ is a notional normal velocity for the boundary, evaluated at the point K, and chosen to preserve the total mass outflow condition. This gives,

$$\bar{U}^* = \frac{1}{S}\int_{K_1}^{K_2} U_n^* \, dS \qquad (7)$$

where the integration is performed over the curved surface K_1BCDK_2 but S is the area corresponding to the straight line segment K_1KK_2.

The mass balance equation (6) is similar in form to the standard equation for an internal cell (1) except for the presence of extra geometric factors, and the replacement of the m_3^* term by one involving the structure motion. Note that for consistency in (6) updated structure velocities are needed in (7), but these are unknown.

Simplest is to use start-of-cycle values instead, so that in place of (7) we would have

$$\bar{U}^* \sim \bar{U} = \frac{1}{S}\int_{K_1}^{K_2} U_n \, dS \qquad (8)$$

This is the basis of the explicit or weak coupling method. By substituting the momenta m_1^*, m_2^*, m_4^* in (6) using (2) and similar momentum equations, a modified pressure equation of the type (4) is derived with the A_3 term absent. The equation is solved by iteration just as for internal cells.

The shortcomings of the explicit coupling method were evidenced in the last Section. It proves futile to update the structure velocities by extrapolation using the start-of-cycle accelerations. In fact, the onset of instability for the free disc problem is sharpened considerably as a result of this.

A new coupling algorithm is now derived based on ideas originally developed for the finite difference thin shell model in SEURBNUK. This model was written specifically for SEURBNUK but with a little adaption the fluid-structure coupling technique is readily generalised for use with EURDYN.

With reference to Figure 4, the accumulated normal force on a given structure node K is separated into that part which derives from the action of the face pressures, and that due to internal (and body) forces.

In general, different time steps are used for the fluid and structure integrations, so that at the nth subcycle of the structure calculation we may express the nodal acceleration as

$$a_k^n = (FP_k^n + FI_k^n)/m_k \qquad (9)$$

in which FP, FI refer to pressure and internal forces respectively, and m_k the nodal mass. With

$$N = \Delta t/\delta t$$

the ratio of the fluid and structure time steps, we take

$$FP_k^n = FP_k^N \quad (= FP_k^*), \qquad FI_k^n = FI_k^0 \quad (= FI_k). \tag{10}$$

That is, end of (fluid) cycle values are assumed for the pressure forces during the N structure time steps, and start of (fluid) cycle values for the internal forces. In other words, pressure forces are treated implicitly, and internal forces explicitly, during the structure calculation. This maintains the consistent use of updated pressures within the code.

In EURDYN, nodal velocities are updated at the nth subcycle according to

$$U_k^n = U_k^{n-1} + \frac{\delta t}{2}(a_k^n + a_k^{n-1}). \tag{11}$$

Using (9), (10) this becomes

$$U_k^n = U_k^{n-1} + \delta t(FP_k^* - FI_k)/m_k$$

with solution

$$U_k^n = U_k + n\ \delta t(FP_k^* - FI_k)/m_k \tag{12}$$

We now define a notional normal velocity U_k^* which when applied over the fluid time step would lead to the same structure displacement as that accumulated during the N subcycles. That is,

$$\Delta t U_k^* = \sum_{n=1}^{N} U_k^n\ \delta t. \tag{13}$$

Using (12), and performing the summation, we find

$$U_k^* = U_k + (\frac{N+1}{2N})\Delta t\left[\frac{FP_k^* - FI_k}{m_k}\right] = U_k + (\frac{N+1}{2N})\Delta t\left[\frac{FP_k^*}{m_k} + a_k - \frac{FP_k}{m_k}\right] \tag{14}$$

the second equality following from (9).

Thus we arrive at an expression for the updated structure normal velocity for use in equation (7). It remains to relate the quantity FP_k^* to the fluid pressures. Again referring to Figure 4, the pressure force acting on the node K is derived from the face pressures on the adjoining half-element faces, as shown. This gives, with the notation in the Figure,

$$FP_k^* = 2\pi\left\{\frac{(r_{k-1} + 3r_k)L_1 + (3r_k + r_{k+1})L_2}{8}\right\}(p_L^* - p_R^*)_k = G_k(p_L^* - p_R^*)_k \tag{15}$$

Combining (14), (15) and performing the integration in (7) we have, averaging the pressure drop along K_1K_2:

$$\bar{U}^* = \Delta t\left\{G(p_L^* - p_R^*) + H\right\} \tag{16}$$

where

$$G = \frac{1}{S}\int_{K_1}^{K_2} (\frac{N+1}{2N})G_k\, dS\ , \qquad H = \frac{1}{S}\int_{K_1}^{K_2}\left\{\frac{U_k}{\Delta t} + (\frac{N+1}{2N})(a_k - \frac{FP_k}{m_k})\right\} dS \tag{17}$$

Equation (16) implicitly relates the end of cycle structure velocity to the fluid pressure field and, with p_L^* (and p_R^*, for thin shells) related back to the grid pressures via appropriate extrapolation formulae, is used in the mass continuity equation (6) to derive a pressure equation for the cell similar to (4). The result is a stable consistent coupling between the fluid and structure calculations, implicit for the pressure derived forces and explicit for the others. With only minor changes to SEURBNUK and EURDYN, the new coupling algorithm was implemented as the standard option for the program. Application to the free

disc problem leads now to the stable solution given in Figure 1.

A number of further numerical experiments have been performed to validate the coding and to verify numerical stability in the presence of pressure wave propogations and restoring forces. These are described in the next Section.

4. FURTHER ONE-DIMENSIONAL TESTS

(a) THE FREE-PLUG PROBLEM

This configuration, shown in Figure 5, comprises a similar shock-tube arrangement as used for the free-disc problem except that the disc is replaced by a free sliding plug. In order to follow pressure wave propogation effects several elements are used across the plug thickness and the fluids are this time treated as compressible. The pressures on the front and back faces of the plug calculated using SEURBNUK-EURDYN are given as functions of time in the Figure, these depicting the pressure propogations along the liquid columns. The pressure drop between the faces drives the plug motion but despite the complex wave interactions the plug displacement follows very closely the analytical solution based on solid body motion.

(b) THE DOUBLE RING PROBLEM

The third test is in radial geometry and based on Test Problem 2a of Phase 3 of the APRICOT code comparison exercise /10/, see Figure 6. An annulus of liquid is bounded externally by a deforming ring in a state of plane strain, and internally by a gas region maintained at constant pressure. In our case a second deforming ring, also in plane strain, is inserted midway between the axis of symmetry and the outer ring. With the liquid treated as incompressible an analytic solution is readily derived which, for the parameters and dimensions chosen, gives the displacement of the inner ring as

$$\xi = 37(1 - \cos 883t) \ \mu m$$

with the time t measured in μsec. The SEURBNUK-EURDYN results for a few oscillations are shown in Figure 6. Notwithstanding the degree of numerical damping due to the rather course spacial discretisation chosen for the problem, the solution is stable and the period of oscillation is well predicted.

5. CONCLUSIONS

A fluid-structure coupling algorithm has been derived which links the implicit fluid dynamics code SEURBNUK with the explicit finite element structures code EURDYN. The formulation implicitly connects the fluid and structure calculations for the pressure derived forces, while the internal structural and body forces are treated explicitly. Stable solutions have been obtained for a number of one-dimensional test cases and in other applications of the code to more complex geometries, for example /11/, /12/, no further instability problems have been encountered.

6. REFERENCES

/1/ CAMERON et al "The Computer Code SEURBNUK-2 for Fast Reactor Explosion Containment Studies, Paper B2/1, SMiRT-4, San Francisco (1977).

/2/ STANIFORTH,R. YERKESS,A. "The Computer Code SEURBNUK-2: Recent Developments", Paper E1/1, SMiRT-5, Berlin (1979).
/3/ SMITH,B.L. YERKESS,A. ADAMSON,J. "Status of the Coupled Fluid-Structure Dynamics Code SEURBNUK", Paper B9/1, SMiRT-7, Chicago (1983).
/4/ HARLOW,F.H. AMSDEN,A.A. "A Numerical Fluid Dynamics Calculation Method for All Flow Speeds", J.Comp.Phys., 8, 197 (1971).
/5/ DONEA,J. GIULIANI,S. "EURDYN, Finite Element Codes for Dynamic Analysis of Large Displacement, Small Strain Problems with Material Non-Linearities", Paper M2/5, SMiRT-3, London (1975).
/6/ DONEA,J. et al "Theoretical Aspects of the EURDYN Computer Programs for Non-Linear Transient Dynamic Analysis of Structural Components", EUR 5473e, JRC Ispra (1976).
/7/ BELYTSCHKO,T. "Methods and Programs for Analysis of Fluid-Structure Systems", Nucl. Eng. Des., 42, 41 (1977).
/8/ WANG,C.Y. "ICECO - An Implicit Eulerian Method for Calculating Fluid Transients in Fast Reactor Containments", ANL-75-81 (1975).
/9/ BELYTSCHKO,T. HSIEH,B.J. "Non-linear Analysis of Shells of Revolution by Convected Co-ordinates", AIAA Journal, 8, 1031 (1974).
/10/ WEST,P.H. HOSKIN,N.E. "APRICOT - Phase 3. Suggested Simple Test Problems for Examination of Thin Shell Modelling and Fluid Structure Coupling", AWRE/44/92/16 (1980).
/11/ SMITH,B.L. et al "A Code Comparison Exercise Based on the LMFBR Containment Experiment MARA-04", Paper E4/7, SMiRT-8, Brussels (1985).
/12/ FICHE,C. et al "Theoretical-Experimental Study of Flexible Roof Effects in an HCDA Simulation", Paper E4/5, SMiRT-8, Brussels (1985).

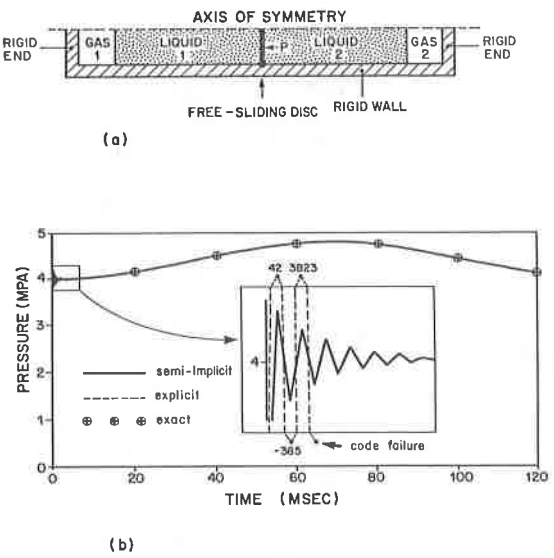

Figure 1 : The Free-Disc Problem
(a) Test Configuration
(b) Pressure History on Rear Face of Disc

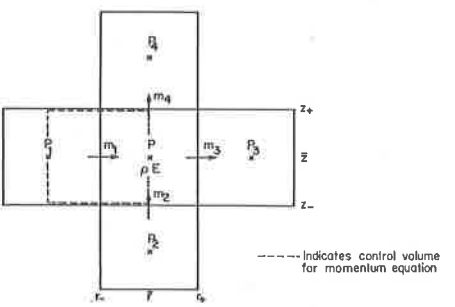

Figure 2 : Placement of the Dependent Variables for an Internal SEURBNUK Cell

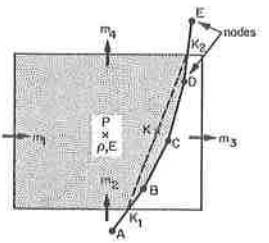

Figure 3 : Fluid-Structure Boundary Cell

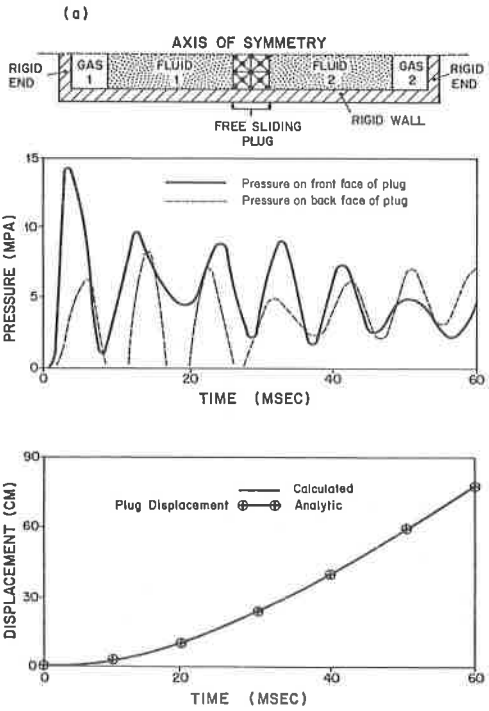

Figure 4 : Node Numbering on a EURDYN Boundary

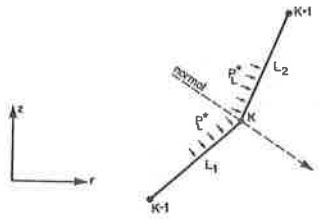

Figure 5 : The Free-Plug Problem

(a) Test Configuration

(b) Face Pressures

(c) Displacement Histories

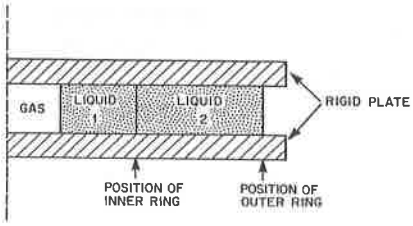

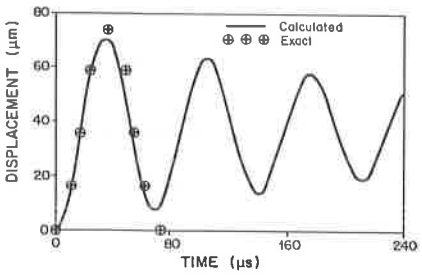

Figure 6 : The Double Ring Problem

(a) Test Configuration

(b) Inner Ring Displacement History